Autonomous Locomotion of Multi-link Mechanical Systems via Natural Oscillation Pattern

Zhiyong Chen, Lijun Zhu, and Tetsuya Iwasaki

Abstract— We consider a class of mechanical systems arising from the dynamics of multi-segmental animal locomotion. Our earlier paper has revealed that a chain of body segments oscillate in a natural mode if the head is externally forced to move at a constant velocity and the damping effect is reduced by an appropriate amount. In this paper, we further show that the natural oscillations, in turn, generate a stable forward velocity (of the head) through a rectification mechanism. As a result, an autonomous locomotion behavior is obtained.

Index Terms— Oscillations, locomotion, robotics, neuronal control, autonomous vehicles

I. INTRODUCTION

Diverse patterns are observed in rhythmic body movements during animal locomotion. Flying eagles and bees have different flapping frequencies, whereas walking adults and children have different strides. It is conjectured that the energy consumption during locomotion is minimized by exploiting the mechanical resonance between the body and the surrounding environment [1], [2]. The idea of resonance exploitation [3]–[7] will be useful for designing efficient robotic locomotors that are robust against and adaptive to environmental changes. However, underlying control mechanisms are largely unknown.

This paper aims at proposing a systematic approach to uncover these mechanisms on a platform of multi-link mechanical systems described by two differential equations:

$$J\ddot{\theta} + D\dot{\theta} + K(v)\theta = u \qquad (1)$$
$$\dot{v} + \xi(\theta)v + \varphi(\theta, \dot{\theta}, \ddot{\theta}) = 0. \qquad (2)$$

The system composed of (1) and (2) is an engineering analogue of various locomotion behaviors of multi-segmental animals including snake, leech, octopus, jellyfish, etc. In this model, $\theta \in \mathbb{R}^n$ is a link angle vector representing the segmental states and $v \in \mathbb{R}^m$ is the locomotion velocity of the body (e.g., the center of gravity or the head). More specifically, the first equation shows how the change

Z. Chen and L. Zhu are with the School of Electrical Engineering and Computer Science, The University of Newcastle, Callaghan, NSW 2308, Australia zhiyong.chen@newcastle.edu.au, c3104718@uon.edu.au

T. Iwasaki is with the Department of Mechanical and Aerospace Engineering, University of California, Los Angeles, CA 90095, USA, tiwasaki@ucla.edu

in the body shape (θ) results from the interaction with environment (represented by the velocity v with respect to the inertial frame) and the body actuation (represented by the torque vector u applied on the links). The second equation, on the contrary, shows how the body shape (θ) resulting from the first equation is rectified to a forward locomotion velocity v. These two equations are coupled to form control principles for animal locomotion as designed by nature and for autonomous robotic locomotors in engineering perspective [8]. Throughout this paper, we call the equations (1) and (2) an oscillation equation and a rectifier equation, respectively. The investigation for the control principles behind these two equations is separated into three tasks as elaborated below.

First, we shall extend the notion of natural oscillations to mechanical systems arising from body-environment interactions during animal or robotic locomotion. It is shown that the system becomes marginally stable, thereby defining a natural oscillation, if the damping effect is adjusted by a proper amount. The second task is to design a controller to achieve the natural oscillation for the closed-loop system. Biological control mechanisms for animal locomotion are known to consist of neuronal circuits, called central pattern generators (CPG) [9]–[11]. A CPG can be modeled as a nonlinear oscillator, and when placed in a feedback loop, provides a basic control architecture to achieve coordinated oscillations of engineered systems [12]–[14]. Therefore, we shall define a class of nonlinear feedback controllers whose architecture is inspired by CPGs.

The aforementioned two tasks are formulated on the oscillation equation (1) only, to show how a natural oscillation pattern is defined and achieved under a specific imposed velocity v. These tasks have been accomplished in [15]. As an example, a scenario was considered where a leech body was dragged forward by an external force with a constant velocity and oscillated as a result of the interactive force from the environment. In reality, however, the velocity v is not applied on the system externally, but is generated by the system itself. In the third task to be studied in this paper, we will move to the coupling structure between the oscillation equation (1) and the rectifier equation (2) to investigate how a locomotion with a natural oscillation pattern can be generated autonomously. As a

result, the control principles underlying the class of multi-link mechanical systems are fully investigated.

The remaining sections of this paper is organized as follows. In Section II, we give the full system model and revisit the definition of natural oscillation and the entrainment controller. The control principles for the class of multi-link mechanical systems are completely studied in Section III by investigating a self-generated locomotion velocity. Finally, the paper is concluded in Section IV.
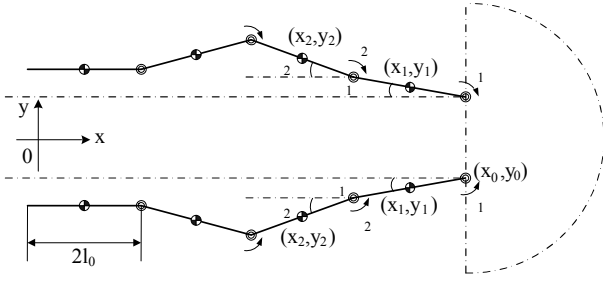
II. Entrainment to Natural Oscillation

Fig. 1. A multi-segmental system with symmetric mechanical structure moving in x-axis only.

As an example of the class of mechanical systems described by (1) and (2), consider a multi-segmental system with a symmetric mechanical structure as shown in Fig. 1. We assume the two chains of multiple links are connected by flexible joints, subject to environmental forces with directional preference, and they undulate symmetrically about the x-axis such that the system moves along the x-axis only. Let (x_o, y_o) be the coordinates of the head, and $v := \dot{x}_o$ be the head velocity resulting from the undulation.

For the system (1) we impose the following:

Assumption 2.1:

(a) $J, K \in \mathbb{R}^{n \times n}$ and $J = J^\mathsf{T} > 0$.

(b) $D = \mu J$ for some $\mu \in \mathbb{R}$.

(c) All the eigenvalues of $J^{-1}K$ are simple and have positive real parts.

The stiffness matrix K is not necessarily symmetric, which is typically given by

$$K(v) = K_o + v\Lambda$$

where K_o is a symmetric positive definite matrix representing the body stiffness, and $v\Lambda$ is an asymmetric matrix representing the skewed stiffness arising from the locomotion at velocity v relative to the environment. For the system given in Fig. 1, we assume there are n identical links in each chain, and each link has mass m_o, length $2l_o$ and moment of inertia $m_o l_o^2/3$, and each joint has torsional stiffness k_o. The angle between the ith link and the negative x-axis is denoted by θ_i. Let τ_i be the torque applied at the ith joint. The environmental force on each

link is modeled as $f_n = -\mu_n v_n$ and $f_t = -\mu_t v_t$, where f_n and f_t are the force components in the direction tangent and normal to the link, v_n and v_t are the components, in the respective directions, of the velocity of the link gravity center, and μ_n and μ_t are proportionality constants [16]. The equations (1) and (2) are developed with (see [8], [15], [16] for the detailed derivation)

$$J = m_o l_o^2(FF^\mathsf{T} + I/3), \ D = (\mu_n/m_o)J,$$
$$K = v\Lambda + k_o BB^\mathsf{T}, \ u = B\tau, \quad \Lambda = l_o(\mu_n - \mu_t)F,$$

$$B = \begin{bmatrix} 1 & -1 & & \\ & \ddots & \ddots & \\ & & 1 & -1 \\ & & & 1 \end{bmatrix}, \ F = \begin{bmatrix} 1 & 2 & \cdots & 2 \\ & 1 & \ddots & \vdots \\ & & \ddots & 2 \\ & & & 1 \end{bmatrix},$$

and

$$\xi(\theta) = c + \theta^\mathsf{T} C\theta$$
$$\varphi(\theta, \dot{\theta}, \ddot{\theta}) = \dot{\theta}^\mathsf{T} S\dot{\theta} + \theta^\mathsf{T} S\ddot{\theta} + \dot{\theta}^\mathsf{T} Q\theta$$
$$c = c_t, \ C = c_n I/n, \ c_t := \mu_t/m_o, \ c_n := \mu_n/m_o$$
$$S = (l_o/n)\text{diag}(Fe), \ Q = (l_o/n)((c_n - c_t)F + c_t S)$$

where v is the head velocity, and $e \in \mathbb{R}^n$ is the vector with all its entries being one.

For a fixed velocity v, we call the system (1) a fliptail locomotor since it is expected to maintain velocity v by flipping (or undulating) the link chain. In [15], we gain insights into the locomotion mechanism by reversing the cause/effect and asking the following: if the head is forced to move at a constant velocity v, would the tail naturally tend to oscillate? A natural oscillation is thus defined as a free response of the modified system obtained by removing a certain damping effects to achieve marginal stability for sustained oscillations. The definition is cited below.

Definition 2.1: Consider the system described by (1) with Assumption 2.1. Let the damping effect be adjusted by a parameter $\epsilon \in \mathbb{R}$ and define the modified system with no input:

$$J\ddot{\theta} + (\mu - \epsilon)J\dot{\theta} + K\theta = 0. \tag{3}$$

If this system has a nonzero characteristic root on the imaginary axis $\lambda = \pm j\omega$ with associated mode shape z for a specific value $\epsilon := \rho$, then the corresponding natural motion of (3) is called a *natural oscillation* (ω, z) of the original system (1) *with damping factor* ρ, where ω and z are referred to as the *natural frequency* and *mode shape* of the natural oscillation.

The natural oscillation can be explicitly calculated using the following lemma given in [15].

Lemma 2.1: *Consider the system in (1) with Assumption 2.1. Let $\omega, \rho \in \mathbb{R}$ and $z \in \mathbb{C}^n$ be given. Then, (ω, z)*

is a natural oscillation of (1) with damping factor ρ if and only if $(\omega, z, \rho) \in \mathbb{N}$ where

$$\mathbb{N} := \{(\omega, z, \rho) \in \mathbb{R} \times \mathbb{C}^n \times \mathbb{R} : \omega = \sqrt{\Re(\varsigma)},$$
$$\rho = \mu + \frac{\Im(\varsigma)}{\sqrt{\Re(\varsigma)}}, \ (\varsigma, z) \in \mathbb{M} \}$$

and $\mathbb{M}$ is the set of generalized eigenvalue/eigenvector pairs of (J, K):

$$\mathbb{M} := \{(\varsigma, z) \in \mathbb{C} \times \mathbb{C}^n : (\varsigma J - K)z = 0\}.$$

To realize the natural oscillation (w, z) for the mechanical system (1), we designed controllers in the following damping augmentation feedback form ([15]):

$$u = \epsilon J\dot{\theta} + w \qquad (4)$$

where w is the new input after the augmentation. The idea is to choose $\epsilon < \varrho$ so that the augmented system is stable, and then apply a sinusoidal input w at the natural frequency ω with appropriate amplitudes and phases to drive the stable system so that the response converges to the natural oscillation with the prescribed amplitude in the steady state. The input w is to be generated by a nonlinear feedback controller of the following form:

$$w = G\psi(q), \quad q = f(s)H\theta \qquad (5)$$

where G and H are $n \times n$ real matrices, $f(s)$ is a scalar transfer function, and ψ is a static nonlinearity satisfying the following properties:

- ψ is odd, bounded, and strictly increasing.
- $\psi(x)$ is strictly concave on $x > 0$, and $\psi'(0) = 1$.

The structure in (5) is motivated by biological control mechanisms. In particular, the simplest input-output model of neuronal dynamics is given by $v_{\text{post}} = \psi(f(s)v_{\text{pre}})$ from the presynaptic potential v_{pre} to the postsynaptic potential v_{post} where ψ and $f(s)$ represent the threshold nonlinearity and dynamics (time lag, adaptation, etc.) associated with synaptic and cell membrane processes. The controller in (5) is a network of multiple neurons with the interconnections specified by G and H.

Theorem 2.1: *Consider the system (1) with Assumption 2.1. For a given $v \in \mathbb{R}$, let $(\varsigma, z) \in \mathbb{M}$ be an optimizer for*

$$\varrho := \min_{(\varsigma, z) \in \mathbb{M}} \mu + \frac{\Im(\varsigma)}{\sqrt{\Re(\varsigma)}}, \qquad (6)$$

and let $\omega := \sqrt{\Re(\varsigma)}$. Then (ω, z) is the natural oscillation with damping factor ϱ, whose oscillation orbit is given by

$$\mathbb{O} := \{ (\vartheta(t), \dot{\vartheta}(t)) \in \mathbb{R}^n \times \mathbb{R}^n \mid t \in \mathbb{R} \},$$
$$\vartheta(t) := Z\cos(\omega t + \phi), \quad Ze^{j\phi} := z.$$

Choose $\epsilon, \eta \in \mathbb{R}$ such that

$$0 < \omega(\varrho - \epsilon) < 1, \quad \varrho - \epsilon = \kappa(\eta\omega)\eta, \quad \eta > 0$$

where κ is the describing function of ψ, and consider the controller

$$u = \epsilon J\dot{\theta} + JZ\psi(\eta Z^{-1}\dot{\theta}).$$

Then, the controller is expected to achieve the entrainment to the natural oscillation (ω, z) in the sense that the trajectory of the closed-loop system $\theta(t)$ converges to the orbit $\mathbb{O}$, i.e., there exists t_o, dependent upon the initial condition, such that

$$\lim_{t \to \infty} \theta(t) - \vartheta(t - t_o) \approx 0.$$

In this above development, we reverse the cause/effect by decoupling the systems (1) and (2) and assuming the head is externally forced to move at a constant velocity v. In fact, v is self-generated through the rectification procedure in (2). Next, we will show that how a stable velocity v is generated with the natural oscillation such that a robotic locomotion occurs autonomously.

III. AUTONOMOUS LOCOMOTION

In the previous section, the natural oscillation is defined and achieved by CPG controllers for a fixed velocity v which is enforced externally. In fact, the more interesting part of the locomotion system is that the persisting natural oscillation, in turn, generates a forward velocity through the rectifier equation (2). In other words, once the damping is compensated by the CPG controllers designed in the previous section, the closed-loop system generates an autonomous locomotion of natural oscillation pattern in a desired forward velocity.

In this section, we will investigate how a stable forward velocity can be self-generated by the locomotion system under a controller designed to achieve a natural oscillation. Recall that the dynamics of the forward velocity is given by (2). To facilitate the analysis of the complete system composed of (1) and (2), let us introduce the following.

Assumption 3.1: A feedback controller has been designed for (1) such that, when the velocity v slowly varies in the neighborhood of v_o, the trajectory of the closed-loop system closely tracks the natural oscillation, with the smallest damping factor ϱ, associated with v.

This assumption may not be satisfied exactly for the controller described in Theorem 2.1 since it is designed for a given constant velocity v. However, numerical simulations will later show that the theory, to be developed under the assumption, works in concert with the controller.

Under Assumption 3.1, for a natural oscillation (ω, z), depending on the velocity v, we can assume $\theta(t) = \Re(ze^{j\omega t})$, and hence,

$$\dot{\theta}(t) = \Re(j\omega z e^{j\omega t}) + \delta_1(\dot{z}, \dot{\omega})$$
$$\ddot{\theta}(t) = \Re(-\omega^2 z e^{j\omega t}) + \delta_2(\dot{z}, \dot{\omega}, \ddot{z}, \ddot{\omega})$$

for some terms δ_1 and δ_2 vanishing at $(\dot{z}, \dot{\omega}, \ddot{z}, \ddot{\omega}) = 0$. Then, some direct calculation is given below:

$$
\begin{aligned}
\|\theta\|^2 &= \|z\|^2/2 + |z^\mathsf{T}|^2 \cos(2(\phi + \omega t))/2 \\
\dot{\theta}^\mathsf{T} S \dot{\theta} + \theta^\mathsf{T} S \ddot{\theta} &= -\omega^2 |z^\mathsf{T}|^2 S \cos(2(\phi + \omega t)) \\
&\quad + \delta_1^\mathsf{T} S \delta_1 + \dot{\theta}^\mathsf{T} S \delta_1 + \delta_1^\mathsf{T} S \dot{\theta} + \theta^\mathsf{T} S \delta_2 \\
\dot{\theta}^\mathsf{T} Q \theta &= -\omega |z^\mathsf{T}| \bar{Q} |z|/2 - \omega |z^\mathsf{T}| \tilde{Q}(t) |z|/2 \\
&\quad + \delta_1^\mathsf{T} Q \theta \\
\bar{Q}_{ij} &= Q_{ij} \sin(\phi_i - \phi_j) \\
\tilde{Q}_{ij}(t) &= Q_{ij} \sin(\phi_i + \phi_j + 2\omega t),
\end{aligned}
$$

where $|z|$ is the column vector with entries $|z_i|$ and $|z^\mathsf{T}|^2$ is the row vector with entries $|z_i|^2$. By using this calculation, we can rewrite (2) as

$$
\dot{v}/\|z\|^2 + [\bar{\xi}(v) + \tilde{\xi}(v,t)]v + \bar{\varphi}(v) + \tilde{\varphi}(v,t) = 0 \quad (7)
$$

where

$$
\begin{aligned}
\bar{\xi}(v) &= c_t/\|z\|^2 + c_n/(2n) \\
\tilde{\xi}(v,t) &= c_n |z_o^\mathsf{T}|^2 \cos(2(\phi + \omega t))/(2n) \\
\bar{\varphi}(v) &= -\omega |z_o^\mathsf{T}| \bar{Q} |z_o|/2 \\
\tilde{\varphi}(v,t) &= -\omega^2 |z_o^\mathsf{T}|^2 S \cos(2(\phi + \omega t)) \\
&\quad - \omega |z_o^\mathsf{T}| \tilde{Q}(t) |z_o|/2 - (\delta_1^\mathsf{T} S \delta_1 + \dot{\theta}^\mathsf{T} S \delta_1 \\
&\quad + \delta_1^\mathsf{T} S \dot{\theta} + \theta^\mathsf{T} S \delta_2 + \delta_1^\mathsf{T} Q \theta)/\|z\|^2.
\end{aligned}
$$

Here, we use $z_o := z/\|z\|$ with $\|z_o\| = 1$ which is the normalized eigenvector representing the oscillation phases and relative amplitudes. The quantities, in particular, ω, z_o, and $\bar{Q}$ in the above development, depend on the velocity v, and will be explicitly expressed as $\omega(v)$, $z_o(v)$, and $\bar{Q}(v)$ when the dependence is important.

Clearly, for a given v, $\bar{\xi}(v)$ and $\bar{\varphi}(v)$ are two constants, but $\tilde{\xi}(v,t)$ and $\tilde{\varphi}(v,t)$ are sinusoidally time varying functions of frequency 2ω. With the decomposition of the functions ξ and φ, we can decompose the velocity $v = \bar{v} + \tilde{v}$ in a corresponding manner. Let $\bar{v}$ be governed by the dynamics:

$$
\dot{\bar{v}}/\|z\|^2 + \bar{\xi}(\bar{v})\bar{v} + \bar{\varphi}(\bar{v}) = 0, \quad (8)
$$

then $\tilde{v}$ must be governed by

$$
\begin{aligned}
\dot{\tilde{v}}/\|z\|^2 &= -\bar{\xi}(v)\tilde{v} + [\bar{\xi}(\bar{v}) - \bar{\xi}(v)]\bar{v} \\
&\quad + [\bar{\varphi}(\bar{v}) - \bar{\varphi}(v)] - \tilde{\xi}(v,t)v - \tilde{\varphi}(v,t). \quad (9)
\end{aligned}
$$

We call $\bar{v}$ and $\tilde{v}$ the average velocity and ripple, respectively. Now, it is ready to reach some conclusions based on the dynamics (8) and (9). Since we have $c_n \gg c_t$ in general, we will consider the case with $c_t = 0$ first, and then take the influence of c_t into account later.

Theorem 3.1: *Under Assumption 3.1, the average velocity governed by (8) with $c_t = 0$ locally asymptotically converges to $\bar{v} = v_o$ if $\alpha(v_o) = v_o$ and $\alpha'(v_o) < 1$, where*

$$
\alpha(x) := n\omega(x)|z_o^\mathsf{T}(x)|\bar{Q}(x)|z_o(x)|/c_n.
$$

Proof. The equilibrium point $\bar{v} = v_o$ of (8) is the solution to the following equation:

$$
\bar{v} = -\bar{\varphi}(\bar{v})/\bar{\xi}(\bar{v}) = \alpha(\bar{v})
$$

which is obviously independent of $\|z\|$. Then, we have

$$
\begin{aligned}
\alpha'(v_o) - 1 &= \frac{-\bar{\varphi}'(v_o) + \bar{\varphi}(v_o)\bar{\xi}'(v_o)/\bar{\xi}(v_o) - \bar{\xi}(v_o)}{\bar{\xi}(v_o)} \\
&= \frac{-\hbar(v_o)}{\bar{\xi}(v_o)}
\end{aligned}
$$

by noting $v_o = -\bar{\varphi}(v_o)/\bar{\xi}(v_o)$, where

$$
\hbar(v_o) := \bar{\xi}(v_o) + \bar{\xi}'(v_o)v_o + \bar{\varphi}'(v_o). \quad (10)
$$

Therefore, $\alpha'(v_o) < 1$ is equivalent to $\hbar(v_o) > 0$. The system (8) can be approximated in the neighborhood of $\bar{x} = x_o$ as follows:

$$
\dot{\bar{v}}/\|z\|^2 + \hbar(v_o)(\bar{v} - v_o) = 0, \quad (11)
$$

and the equilibrium point is asymptotically stable if $\hbar(v_o) > 0$ is satisfied, or, $\alpha'(v_o) < 1$. ∎

Remark 3.1: It is shown in Theorem 3.1 that a forward velocity v_o, calculated from $\alpha(v_o) = v_o$, is independent of the oscillation amplitude $\|z\|$, since so is the function $\alpha(x)$. This holds true due to $c_t = 0$.
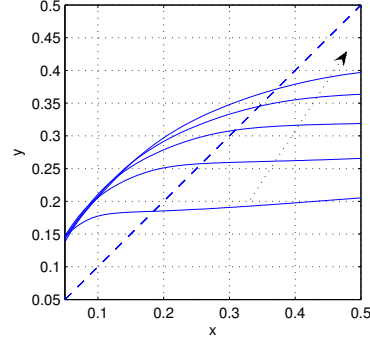

Fig. 2. Solution to $\alpha(x) = x$. The solid curves represent $y = \alpha(x)$ for $\varkappa = 1, 2, 3, 4, 5$, along the arrow, and the dashed line is $y = x$. The intersection $\alpha(x) = x$ occurs at $x = 0.185, 0.257, 0.309, 0.345, 0.372$, respectively.

Example 3.1: Consider a system with the following parameter values: The number of links is $n = 5$, and each link has mass $m_o := m/n$ and length $2l_o = l/n$, where the total length is $l = 0.5$ m and mass is $m = 0.2$ kg. The environmental force constants are $\mu_t = 0$ and $\mu_n = 0.5$ Ns/m, and each joint has stiffness $k_o = 2.5 \times 10^{-4} \varkappa$ Nm/rad, where the parameter $\varkappa$ is used to examine the effect of stiffness perturbation. For different $\varkappa$'s, we can find the solution to $\alpha(x) = x$ in Fig. 2. The result shows
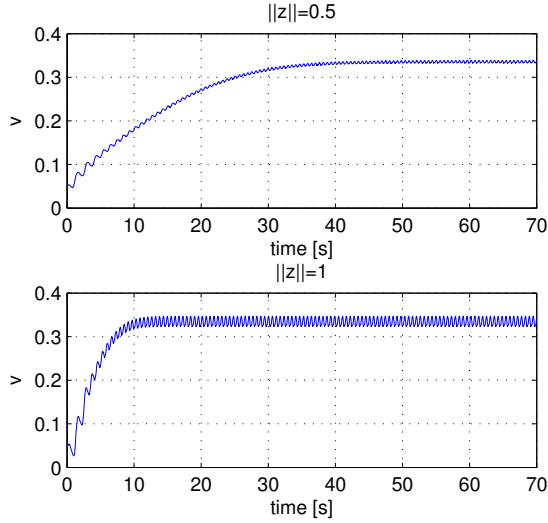
Fig. 3. Self-generated velocity v. The expected velocity $v_o = 0.345$ is effectively achieved with different amplitudes.
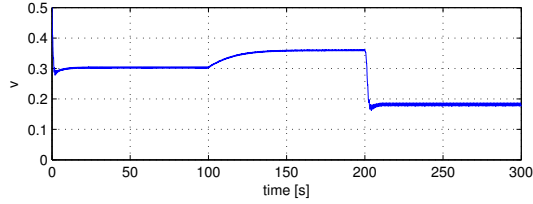

Fig. 4. Forward velocity changes with $\varkappa$ ($\|z\| = 0.5$).

OSCILLATION PROFILES WITH DIFFERENT AMPLITUDES ($\phi_5 = 0°$)

$/$	Period	ϕ_1	ϕ_2	ϕ_3	ϕ_4
natu. osci.	1.12	332°	232°	141°	64°
simu. ($\|z\| = 0.5$)	1.16	328°	229°	139°	63°
simu. ($\|z\| = 1$)	1.16	329°	228°	139°	62°

$\|z\|$	$\|z_1\|$	$\|z_2\|$	$\|z_3\|$	$\|z_4\|$	$\|z_5\|$
0.5 (natu. osci.)	0.90°	3.53°	8.55°	14.77°	22.72°
0.5 (simu.)	0.91°	3.58°	8.71°	15.07°	23.49°
1 (natu. osci.)	1.80°	7.06°	17.10°	29.54°	45.44°
1 (simu.)	1.82°	7.17°	17.25°	30.04°	46.96°

system can achieve the corresponding velocity calculated in Fig. 2.

Remark 3.2: The magnitude of the ripple $\tilde{v}$ is expected to be small if the oscillation amplitude is small. We have shown that the amplitude $\|z\|$ does not affect the forward velocity or the oscillation pattern (frequency and phase). However, it does have a significant effect on the ripple carried in the forward velocity. The ripple $\tilde{v}$ is governed by (9), which, in the neighborhood of $v = \bar{v} = v_o$, is approximated as

$$\dot{\tilde{v}}/\|z\|^2 + \hbar(v_o)\tilde{v} = -\tilde{\xi}(v,t)v - \tilde{\varphi}(v,t) \qquad (12)$$

where $\hbar(v_o) > 0$ is defined in (10). The term $(\delta_1^\mathsf{T} S \delta_1 + \dot{\theta}^\mathsf{T} S \delta_1 + \delta_1^\mathsf{T} S \dot{\theta} + \theta^\mathsf{T} S \delta_2 + \delta_1^\mathsf{T} Q \theta)/\|z\|^2$ in $\tilde{\varphi}(v,t)$ is small when the velocity v slowly varies. Clearly, the term $-\tilde{\xi}(v,t)v - \tilde{\varphi}(v,t)$ can be regarded as a sinusoidal signal with a frequency 2ω (see the definitions of $\tilde{\xi}(v,t)$ and $\tilde{\varphi}(v,t)$), and its output through a low pass filter $f(s) = 1/[\hbar(v_o) + s/\|z\|^2]$ is $\tilde{v}$. The gain of the filter is $|f(j2\omega)|$ and obviously $|f(j2\omega)| \to 0$ as $\|z\| \to 0$, which implies the conclusion. This phenomenon has been demonstrated in Fig. 3 where the magnitude of the ripple is less for $\|z\| = 0.5$ than $\|z\| = 1$. The ripple can be further attenuated if we reduce the oscillation amplitude.

Remark 3.3: The introduction of $\mu_t > 0$ reduces the forward velocity, more significantly for a smaller oscillation amplitude. With a non-zero μ_t, the function $\alpha(\bar{v})$ is redefined as follows:

$$\alpha(\bar{v}) := -\frac{\bar{\varphi}(\bar{v})}{\bar{\xi}(\bar{v})} = \frac{n\omega(\bar{v})|z_o^\mathsf{T}(\bar{v})|\bar{Q}(\bar{v})|z_o(\bar{v})|}{2nc_t/\|z(\bar{v})\|^2 + c_n}.$$

Clearly, the introduction of μ_t reduces $\alpha(\bar{v})$ and hence reduces the equilibrium point v_o, the solution to $\alpha(\bar{v}) = \bar{v}$, more significantly for a smaller oscillation amplitude $\|z\|$.

Example 3.3: Consider the system given in Example. 3.1 with $\varkappa = 4$, but $\mu_t = 0.01$. As calculated in Fig. 5, for $\|z\| = 0.5$ and $\|z\| = 1$, the corresponding equilibrium point is $v_o = 0.097$ and $v_o = 0.242$, respectively. The forward velocity can still be achieved as shown in Fig. 6.

that, to expect a higher velocity, the stiffness of the body must be strengthen.

Example 3.2: Consider the system given in Example 3.1. From Fig. 2, it is easy to see that $\alpha'(v_o) < 1$ is true for all cases. In the other words, all equilibrium points corresponding to $\varkappa = 1, \ldots, 5$ are asymptotically stable. Let us take $\varkappa = 4$ as an example and the simulation result is given in Fig. 3. The expected velocity is $v_o = 0.345$ as calculated in Fig. 2. The simulation on the system composed of (1) and (2) shows that this same velocity can be achieved with different oscillation amplitudes (e.g., $\|z\| = 0.5$ and $\|z\| = 1$) under the idealized condition where $\mu_t = 0$. More importantly, the natural oscillation is also achieved when the velocity occurs as shown in Table. I.

On top of the CPG controllers designed in the previous section, an additional term $\bar{k}BB^\mathsf{T}\theta$ can be added to tune the stiffness from k_o to $k_o + \bar{k}$. By doing this, we can modify the forward velocity of the system for set point tracking. This tracking scenario is demonstrated in Fig. 4 where $\varkappa$ is changed stepwise at $t = 100$ and 200 s to take values $3, 5, 1$ for successive durations. The closed-loop
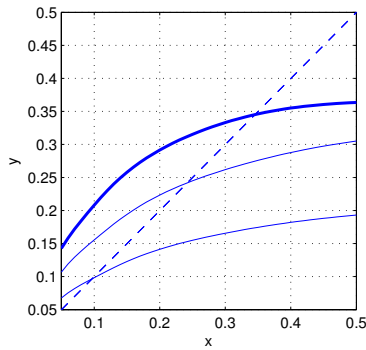
Fig. 5. Solution to $\alpha(x) = x$ with $\mu_t \geq 0$. The bold curve is with $\mu_t = 0$ copied from Fig. 2. The other two curves are for $\|z\| = 0.5$ and $\|z\| = 1$ with $\mu_t = 0.01$ which intersect $y = x$ at $x = 0.097$ and $x = 0.242$, respectively. For all cases, $\varkappa = 4$ is used.
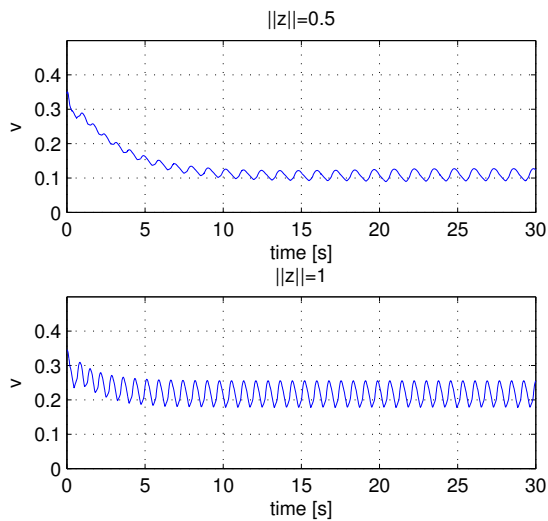

Fig. 6. Self-generated velocity v with $\mu_t = 0.01$. The expected velocities $v_o = 0.097$ and $v_o = 0.242$ are effectively achieved (dropped from $v_o = 0.345$ with $\mu_t = 0$).

IV. CONCLUSION

We have considered a class of mechanical systems characterized by asymmetric stiffness matrices, arising from typical dynamics of animal locomotion. The natural oscillation is defined for such systems as a free response of damping-compensated systems, and is shown to capture rhythmic movements of flipping tails for swimming. The control architectures are inspired by biological mechanisms. Also, the undulatory movement of the body in a natural oscillation pattern induces a stable forward velocity and thus forms an autonomous robotic locomotion.

REFERENCES

[1] G.A. Cavagna, N.C. Heglund, and C.R. Taylor. Mechanical work in terrestrial locomotion: Two basic mechanisms for minimizing energy expenditure. *Am. J. Physiol.*, 233:R243–R261, 1977.

[2] J. Rose and J.G. Gamble. *Human Walking*. Philadelphia, PA: Lippincott Williams and Wilkins, 3rd ed., 2003.

[3] N.G. Hatsopoulos. Coupling the neural and physical dynamics in rhythmic movements. *Neural Computation*, 8(3):567–581, 1996.

[4] T. Iwasaki and M. Zheng. Sensory feedback mechanism underlying entrainment of central pattern generator to mechanical resonance. *Biological Cybernetics*, 94(4):245–261, 2006.

[5] B.W. Verdaasdonk, H.F. Koopman, and F.C. Van der Helm. Resonance tuning in a neuro-musculo-skeletal model of the forearm. *Biological Cybernetics*, 96(2):165–180, 2007.

[6] C.A. Williams and S.P. DeWeerth. A comparison of resonance tuning with positive versus negative sensory feedback. *Biol. Cyb.*, 96:603–614, 2007.

[7] Y. Futakata and T. Iwasaki. Formal analysis of resonance entrainment by central pattern generator. *J. Math. Biol.*, 57(2):183–207, 2008.

[8] J. Blair and T. Iwasaki. Optimal gaits for mechanical rectifier systems. *IEEE Trans. Auto. Contr.*, 2010. (To appear).

[9] T.G. Brown. The intrinsic factors in the act of progression in the mammal. *Proc. Roy. Soc. Lond.*, 84:308–319, 1911.

[10] S. Grillner, J.T. Buchanan, P. Walker, and L. Brodin. *Neural Control of Rhythmic Movements in Vertebrates*. New York: Wiley, 1988.

[11] G.N. Orlovsky, T.G. Deliagina, and S. Grillner. *Neuronal Control of Locomotion: From Mollusc to Man*. Oxford University Press, 1999.

[12] Y. Fukuoka, H. Kimura, and A.H. Cohen. Adaptive dynamic walking of a quadruped robot on irregular terrain based on biological concepts. *Int. J. Robotics Research*, 22(3-4):187–202, 2003.

[13] G. Taga. Self-organized control of bipedal locomotion by neural oscillators in unpredictable environment. *Biol. Cybern.*, 65:147–159, 1991.

[14] M.A. Lewis and G.A. Bekey. Gait adaptation in a quadruped robot. *Autonomous Robots*, 12(3):301–312, 2002.

[15] Z. Chen and T. Iwasaki. Robust entrainment to natural oscillations of asymmetric systems arising from animal locomotion. *Proc. IEEE Conf. Dec. Contr.*, 2009.

[16] M. Saito, M. Fukaya, and T. Iwasaki. Serpentine locomotion with robotic snake. *IEEE Control Systems Magazine*, 22(1):64–81, 2002.